

# Automated Kinetic Imaging Assay of Cell Proliferation in 384-Well Format

Image-based kinetic analysis of cell proliferation and cell death mechanisms

## Author

Rebecca Mongeon, PhD  
Agilent Technologies, Inc.

## Abstract

Evasion of cell death is a hallmark of cancer cells that allows them to overcome endogenous barriers to cancer development, as well as to resist treatment. Understanding how cancer cells are able to evade cell death promises to unlock new avenues to treat human cancer. This application note presents a fully automated image-based assay to monitor both the proliferation and cell death of a fibrosarcoma cancer cell line in response to multiple antineoplastic drugs in a high-throughput format.

## Introduction

Even from the beginning of life, the proper function of all multicellular organisms depends on cell death. Mismanaged cell death underlies phenomena ranging from developmental abnormalities to cancer. The ability of cancerous cells to evade regulated cell death, or apoptosis, is particularly problematic for cancer treatment.<sup>1</sup> Whether through radiation, immunotherapy, or chemotherapy, the goal of cancer treatment is the selective death of the cancerous cells. Understanding the many facets of cell death, and in particular those aspects that cancer cells are able to overcome, is an active area of interest for clinicians, primary researchers and drug discovery efforts alike.<sup>1</sup> Imaging-based tools to monitor cells undergoing different cell death mechanisms have provided a means to probe cell death in a continuous, live, high-throughput manner.

Regulated cell death, such as apoptosis, and accidental cell death, such as necrosis, are both processes that can occur in response to a cellular stressor (i.e. nutrient deprivation or DNA damage), but each produces different hallmark cellular changes.<sup>2</sup> One of the characteristics of early state apoptosis occurs when phosphatidylserine, a membrane component normally only found within the inner leaflet of cell membranes, translocates to the outer leaflet. This exposure of phosphatidylserine likely prompts engulfment of the cell, or remaining cell fragments, by phagocytes.<sup>3</sup> In this application note, phosphatidylserine exposure was optically monitored in live cells through its specific binding and activation of the fluorescent pSIVA-IANBD probe. This fluorescent probe provides a live, kinetic indicator of cells undergoing apoptosis and persists through cell death.<sup>4</sup>

A characteristic change during both late-stage apoptosis and necrosis processes is that cell membrane integrity is lost.<sup>2</sup> This loss of integrity allows molecules that are normally excluded to enter cell nuclei, such as the DNA-staining dye propidium iodide (PI). Therefore, fluorescent PI staining of nuclei can also be monitored in real time as a measure of cells undergoing necrosis and late-stage apoptosis processes.

This study combined long-term kinetic label-free cell counting and fluorescent imaging to monitor cancer cell responses over several days in a high-throughput 384-well image-based assay. The Agilent BioTek Cytation 5 cell imaging multimode reader with a wide field of view camera enables capture of

the entire 384-well in a single image. Coupling the Cytation 5 with the Agilent BioTek BioSpa 8 automated incubator for fully automated environmental control enabled a walk-away workflow of high-throughput image-based cellular analysis.

## Materials and methods

### Reagents

HT-1080 fibrosarcoma cells were obtained from ATCC (Manassas, VA). Advanced DMEM, Fluorobright DMEM, fetal bovine serum (FBS), and glutamine/penicillin/streptomycin were purchased from Thermo Fisher Scientific (Waltham, MA). Staurosporine, nocodazole, nigericin and camptothecin were purchased from Tocris Bioscience (Minneapolis, MN). The Kinetic Apoptosis kit for microscopy (ab129817) was purchased from Abcam (Cambridge, MA). Greiner 384-well microplates (part number 781091) were obtained from Sigma-Aldrich (St. Louis, MO).

### Cell culture and assay preparation

HT-1080 cells were maintained in Advanced DMEM media supplemented with 10% FBS, 2 mM glutamine and penicillin/streptomycin at 37 °C in a humidified incubator with 5% CO<sub>2</sub>. Cells were routinely passaged at 80% confluency. For seeding in 384-well microplates, HT-1080 cells were harvested and suspensions were added at a density of 500 cells per well. After cells adhered (approximately 4 hours), media was exchanged for Fluorobrite DMEM media. The kinetic apoptosis kit reagents were added to each well to a final concentration of 1 μL/mL pSIVA-IANBD and 2 μL/mL PI. Dilution series of antineoplastic drugs were added across the microplate, and imaging was started immediately following drug addition.

### Automated long-term live-cell imaging

For fully automated long-term imaging, cells were maintained in a BioSpa 8 automated incubator that was coupled to a Cytation 5 cell imaging multimode reader with a wide field of view camera. The BioSpa maintained cells at 37 °C, 5% CO<sub>2</sub> and 80 to 90% humidity throughout the course of the 72-hour experiment, and environmental parameters were monitored and reported live through Agilent BioTek BioSpa software. The microplate was automatically transferred from the BioSpa incubator to the Cytation 5 at two-hour intervals for imaging. Additional environmental controls inside the Cytation 5 maintained cells at 37 °C and 5% CO<sub>2</sub> throughout the imaging procedure.

## Single image whole-well capture

For whole-well imaging of the 384-well microplate, the Cytation 5, with wide-field-of-view camera, was paired with a 4x magnification objective. The Cytation 5 wide-field-of-view enabled a single-image capture of the entire culture area of the well (see Figure 1). The Cytation 5 was configured for imaging as shown in Table 1. Imaging cubes GFP (469/525 nm) and PI (531/647 nm) were used for detection of kinetic apoptosis kit reagents pSIVA and PI signals, respectively. For label-free cell counting, the Cytation 5 with high contrast brightfield was used as described previously.<sup>5</sup>

**Table 1.** Agilent BioTek Gen5 software settings for image acquisition.

Image Acquisition	
Parameter	Value
Channel	Brightfield (high contrast) GFP 469,525 Propidium iodide 531,647
Focus	Laser autofocus
Objective	4x PL FL
Z-stack	No
Montage	No
Discontinuous Kinetic Procedure	Yes
Estimated Total Time	3 days
Estimated Interval	2 hours

## Image analysis

Image processing was performed using Agilent BioTek Gen5 software, and the parameters used are listed in Table 2. Preprocessing reduced background and enhanced contrast, readily enabling cell identification in all channels. For the high-contrast brightfield image, processing results in an image with a black background, and bright white spots corresponding to cells.

**Table 2.** Agilent BioTek Gen5 software image processing parameters.

Image Processing			
Parameter	Brightfield	GFP 469,525	Propidium Iodide 531,647
Background	Dark	Dark	Dark
Rolling Ball Diameter	20	100	30
Priority	Fine results	Fine results	Fine results
Image Smoothing Strength	5 cycles	1 cycle	1 cycle

Cellular analysis was performed on preprocessed images and the parameters for all channels used are listed in Table 3. For each channel, the threshold value was determined through the image statistics analysis in Gen5. Image statistics of control wells was carried out, and three standard deviations above the average image signal was used as the threshold value for cellular analysis. Total cell counts were established through primary mask analysis of the high-contrast brightfield image. The number of cells positive for the apoptotic reporter pSIVA was established through primary mask analysis of the GFP channel. The number of cells positive for the necrotic marker, PI, was established through primary mask analysis of the PI channel. The liquid meniscus introduced an imaging artifact where the corners of the square well were slightly less illuminated in brightfield than the rest of the culture area (see Figure 1), potentially introducing bias in the label-free cell counts compared to fluorescence counts. The Gen5 plug feature was used to restrict cellular analysis to the area of the well best illuminated in brightfield (a 3,400  $\mu\text{m}$  diameter circle), corresponding to ~92% of the total well culture area. Therefore, the plug feature enabled unbiased normalization of fluorescent cell counts using label-free cell counting methods.

**Table 3.** Agilent BioTek Gen5 software cellular analysis parameters.

Cellular Analysis			
Parameter	Brightfield Cell Count	pSIVA Count	PI Count
<b>Primary Mask</b>			
Detection Channel	Tsf[Brightfield]	Tsf[GFP 469,525]	Tsf[Propidium Iodide 531,647]
Threshold	8,000	4,000	3,000
Background	Dark	Dark	Dark
Split Touching Objects	Yes	Yes	Yes
Fill Holes in Masks	Yes	Yes	Yes
Minimum Object Size	10 $\mu\text{m}$	15 $\mu\text{m}$	5 $\mu\text{m}$
Maximum Object Size	100 $\mu\text{m}$	100 $\mu\text{m}$	100 $\mu\text{m}$
Include Primary Edge Objects	No	No	No
Analyze Entire Image	No	No	No
<b>Advanced Detection Options</b>			
Rolling Ball Diameter	Auto	50	30
Image Smoothing Strength	3 cycles	3 cycles	3 cycles
Evaluate Background On	5%	5%	5%
Primary Mask	Use threshold mask	Use threshold mask	Use threshold mask

### Curve fitting and statistics

All data were collected and analyzed using Agilent BioTek Gen5 software. For data presentation, both Gen5 and GraphPad Prism V8 software were used. All curve fitting and  $EC_{50}$  analysis was performed in Gen5. Time of  $V_{max}$  analysis in Gen5 was performed over a 5-point window for linear regression. Statistical analysis was performed using the Student's t-test function (two-tailed, unpaired) in Microsoft Excel.

## Results and discussion

### Automated kinetic analysis of proliferation

Label-free image-based cell counting of the human fibrosarcoma cell line HT-1080 was performed at two-hour intervals over three days in a 384-well plate. For each well, a single image was captured using a 4x objective and the high contrast brightfield kit. Cell counts were established using cellular analysis in Gen5 (Figure 1).

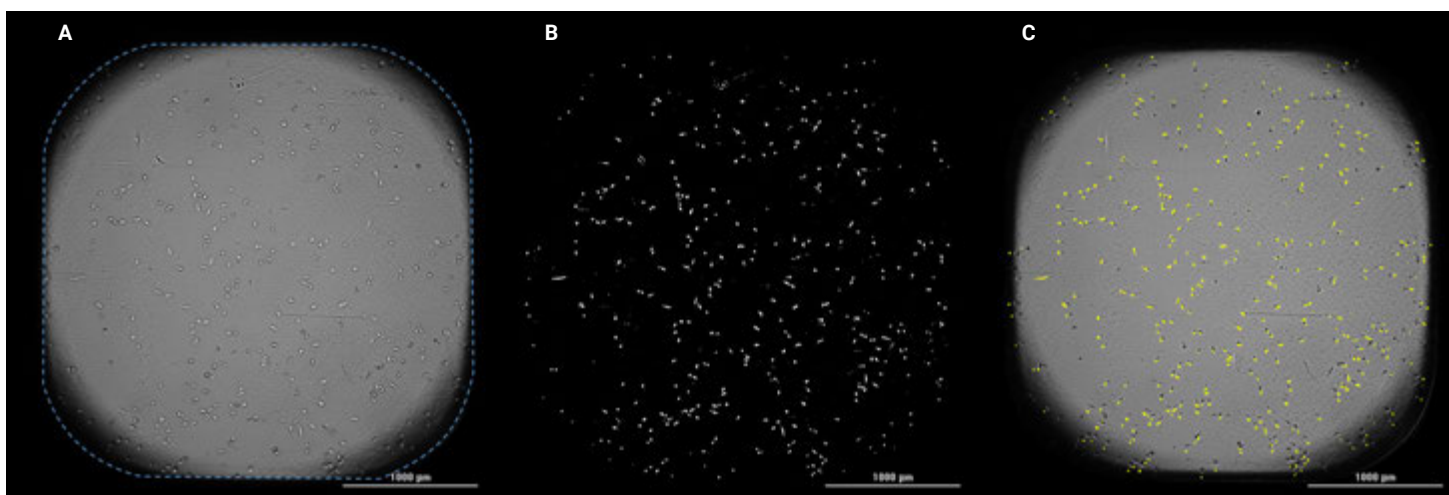


**Figure 1.** Label-free high contrast cell counting method. (A) Original high contrast defocused image captured with the high contrast kit. Total culture area of a single well of the 384-well plate is outlined in dashed blue line. (B) High contrast brightfield image after preprocessing steps indicated in Table 2. (C) Agilent BioTek Gen5 cellular analysis software identifies and counts HT-1080 cells (yellow), shown overlaid on original high contrast brightfield image.

The effect on cell proliferation of four antineoplastic drugs (staurosporine, nocodazole, camptothecin, and nigericin) was examined. The drugs were added just before the first images were acquired at  $t = 0$  hours. Gen5 software generated curves

of cell counts providing a visual overview of proliferation rates for the entire 384-well dish (Figure 2). The differential inhibitory effect of each drug on proliferation was readily appreciated in the Gen5 plate overview.

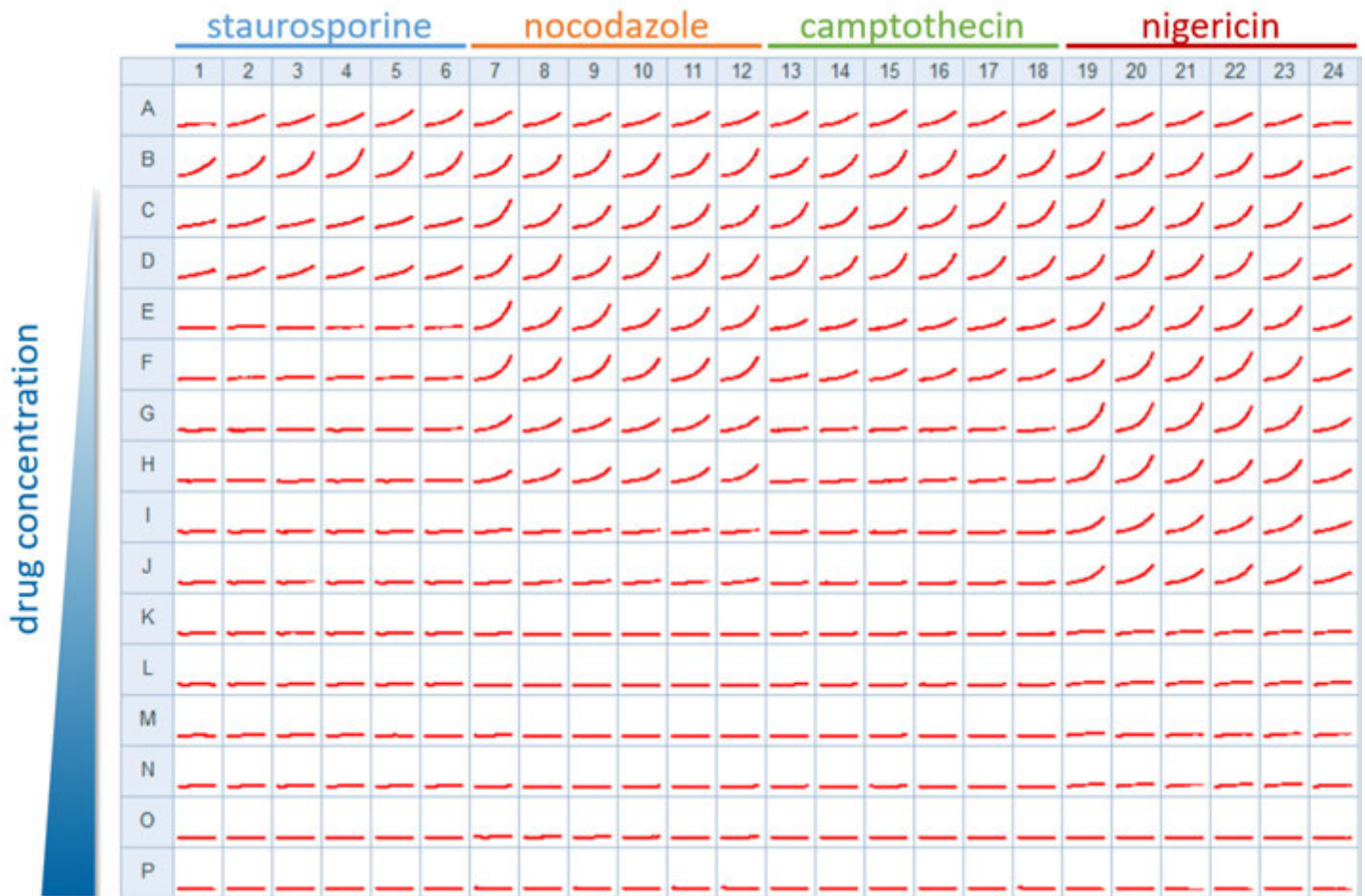


**Figure 2.** 384-well plate overview of cell proliferation. Red curves indicate cell count plotted over the duration of the 3-day experiment. As drug concentration increases from rows C through P, reduced proliferation is observed for all drugs across the entire 384-well plate.

For two example drugs, nocodazole and camptothecin, cell counts are plotted together across the different doses (Figure 3A, 3B). For all further analysis, replicates of 12 wells for each condition were averaged and plotted together. To quantify the inhibitory effect of each drug on proliferation, dose-response curves were generated in Gen5 (Figure 3C, 3D). Dose-response curves were first generated for different drugs through single time point analysis at 24 hours.

Gen5 provides an additional comparison of  $IC_{50}$  values from integral analysis of the area under the curve (Figure 4). This way of calculating  $IC_{50}$  values was independent of drug exposure time, and accounted for changes across the duration of the experiment. For camptothecin,  $IC_{50}$  values were in good agreement between analysis methodologies. For comparison, AUC analysis was also done for nigericin and nocodazole, demonstrating assay sensitivity across large variations in  $IC_{50}$  (Figure 4C).

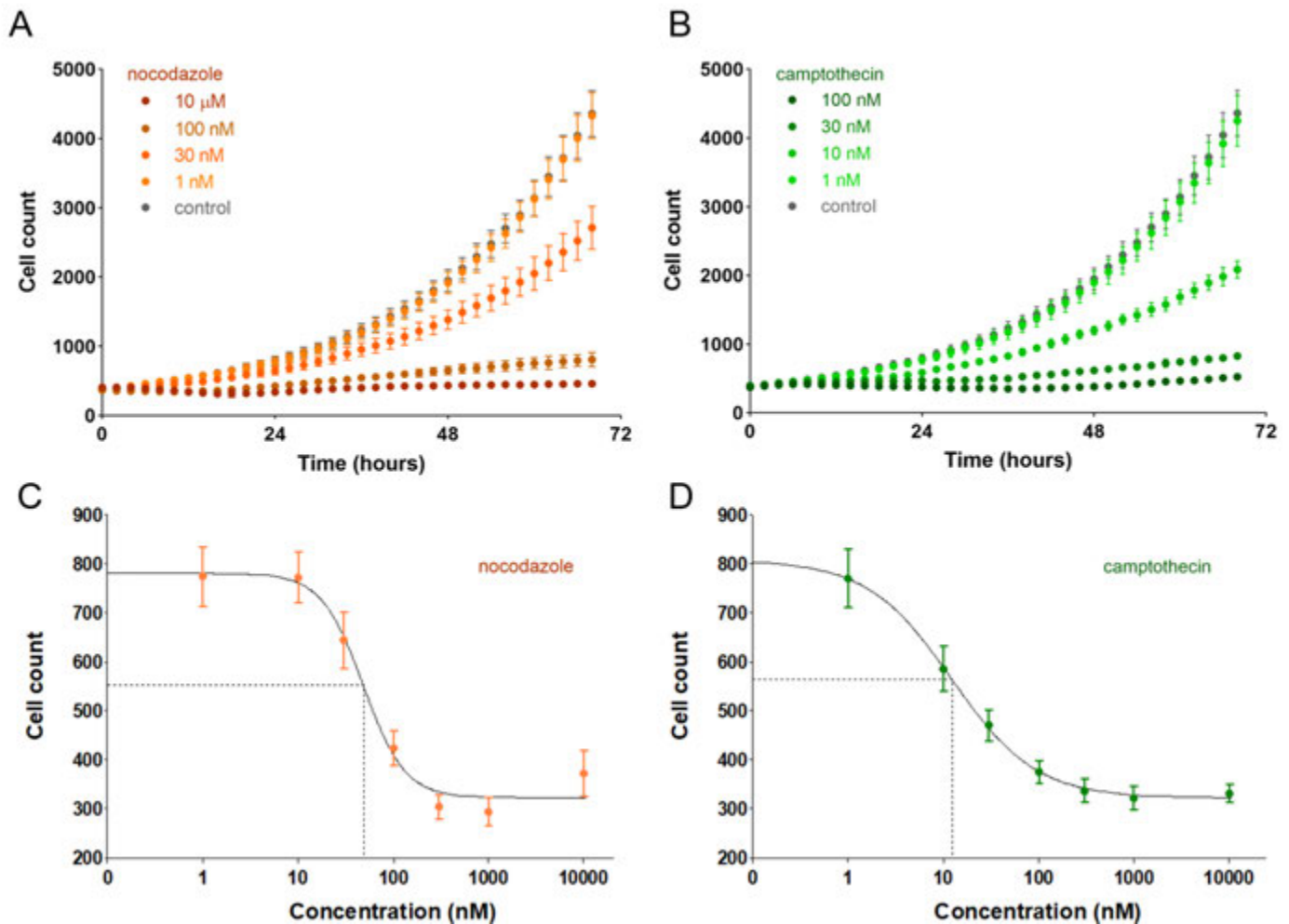


**Figure 3.** Dose-dependent inhibition of HT-1080 fibrosarcoma cell proliferation. Average cell count plots are overlaid for several concentrations of (A) nocodazole (orange circles,  $n = 12$  replicate wells) and (B) camptothecin (green circles,  $n = 12$  replicate wells) over three days. Error bars indicate standard deviation of replicates. Agilent BioTek Gen5 generated dose-response curves for label-free cell counts at a single time point of 24 hours for (C) nocodazole (orange circles) and (D) camptothecin (green circles). The 4-parameter fits are indicated in black solid lines, and interpolated  $IC_{50}$  values are visualized with dashed lines. For nocodazole, the  $IC_{50}$  corresponds to 48 nM, and for camptothecin corresponds to 12 nM.

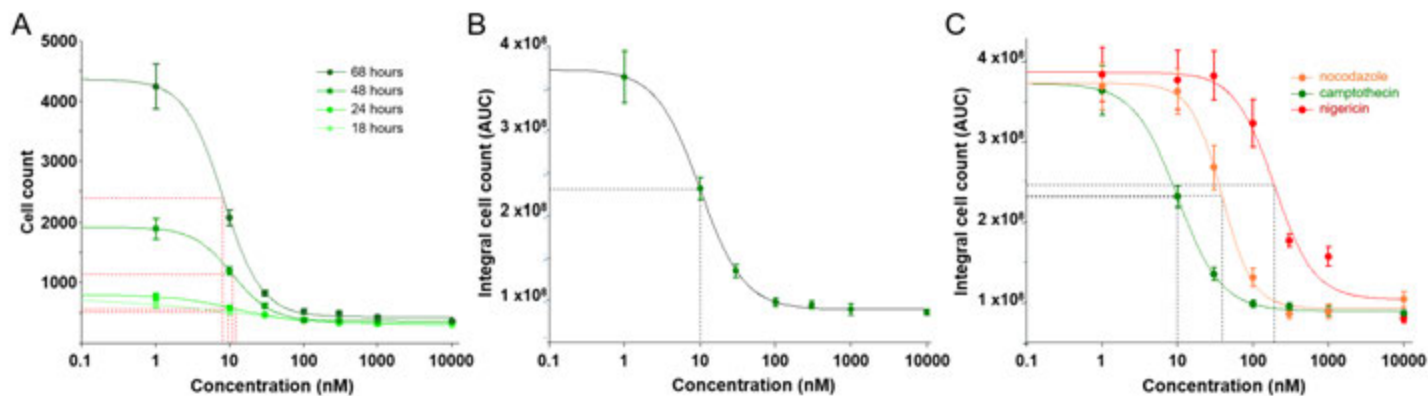


**Figure 4.** Label-free proliferation dose-response curves with  $IC_{50}$  analysis. (A) Dose-response curves for multiple time points are overlaid for camptothecin, allowing time-dependent comparison of  $IC_{50}$  values (18 hours = 9.5 nM, 24 hours = 12.3 nM, 48 hours = 10.9 nM, and 68 hours = 8.2 nM). For each curve the 4-parameter fit is colored and the  $IC_{50}$  interpolation is visualized in dashed lines. (B) Agilent BioTek Gen5 provides additional estimates of  $IC_{50}$  values through area-under-the-curve (integral) analysis for the entire kinetic series ( $IC_{50}$  = 10 nM). (C) Integral-based dose-response curves for three drugs indicated. Solid lines correspond to 4-parameter fit, and dashed lines indicate  $IC_{50}$  interpolation.  $IC_{50}$  values correspond to 10 nM for camptothecin, 39 nM for nocodazole, and 193 nM for nigericin.

### Fluorescence-based kinetic cell death phenotype

In addition to the overall effect on proliferation, the mechanism of cell death was examined using fluorescent reporters of apoptosis and necrosis. At each time point where brightfield images were taken, corresponding fluorescence

images were taken of the apoptosis marker pSIVA and the necrosis marker PI (Figure 5A). Cells were identified positive for pSIVA and PI signals (Figure 5B) and primary masks identified individual cells for each well and time point (Figure 5B, see inset).

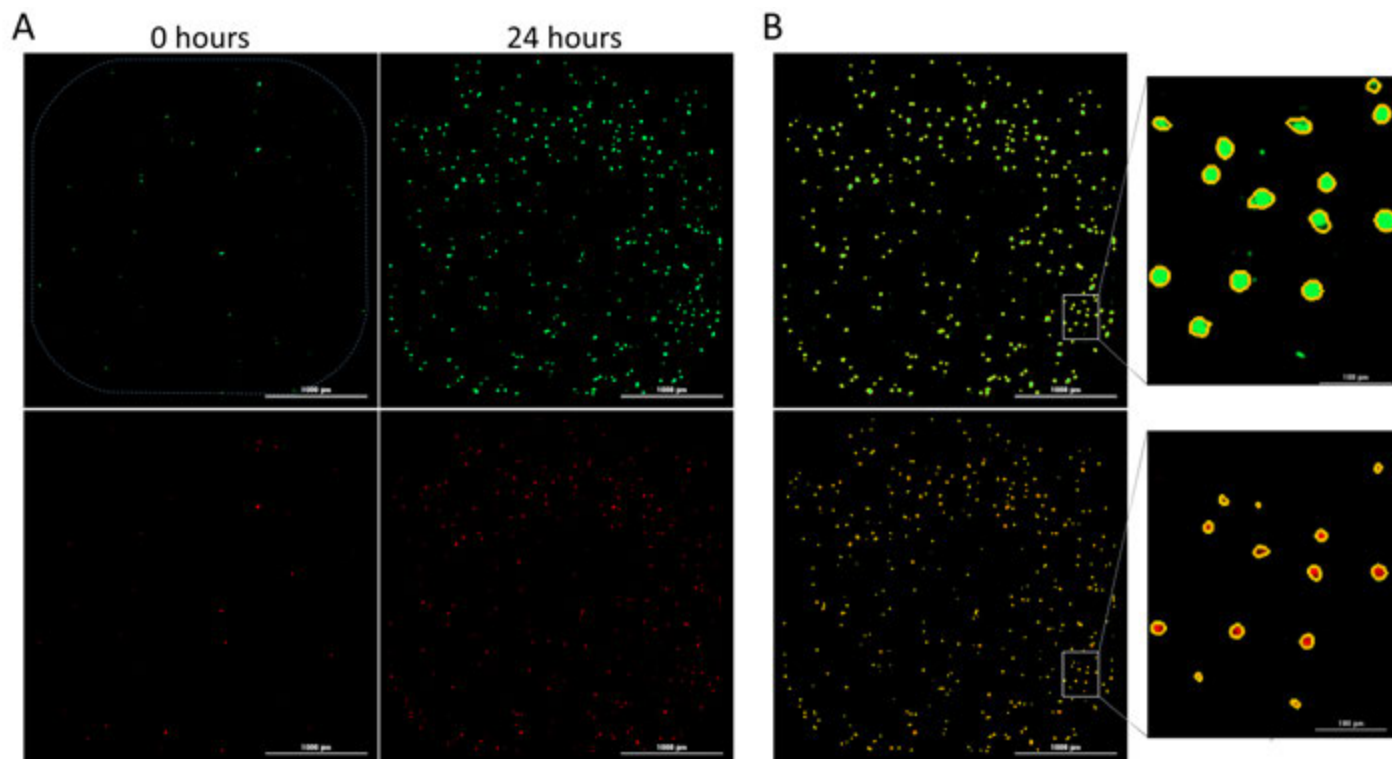


**Figure 5.** Capture and identification of cells positive for apoptosis and necrosis. (A) Example images of cells positive for pSIVA apoptosis marker (green, upper panels) and PI necrosis marker (red, lower panels) at two time points (indicated). The area of the 384-well bottom is indicated by the dashed blue outline in the top left panel of A. (B) Positive apoptotic and necrotic cells were identified by size and signal threshold parameters (see Materials and methods) and primary masks identified positive cells (inset shows enlarged region for clarity).

### Quantitative analysis of apoptosis

The green fluorescence of pSIVA will increase as phosphatidylserine is exposed to the extracellular space. As expected, the number of cells positive for the apoptosis marker pSIVA increases over time in response to antineoplastics, but remains relatively stable at a low level in control wells (Figure 6A). Although the behavior is expected at the highest and lowest concentrations of nocodazole, at intermediate concentrations the number of cells positive for pSIVA continues to increase over time. This accumulation is due to the continued proliferation of the total cell population,

despite the fact that many of the cells are actively undergoing cell death. This effect obscures the interpretation of the results, as well as left-shifts the  $EC_{50}$  value of the resultant dose-response curve over time (Figure 6A, bottom panel).

To control for the continued proliferation of the cells, as well as any initial variability in cell numbers between conditions and replicates, the pSIVA-positive cell counts can be expressed as a percent of total cell counts established through the label-free cell counts. (Figure 6B).

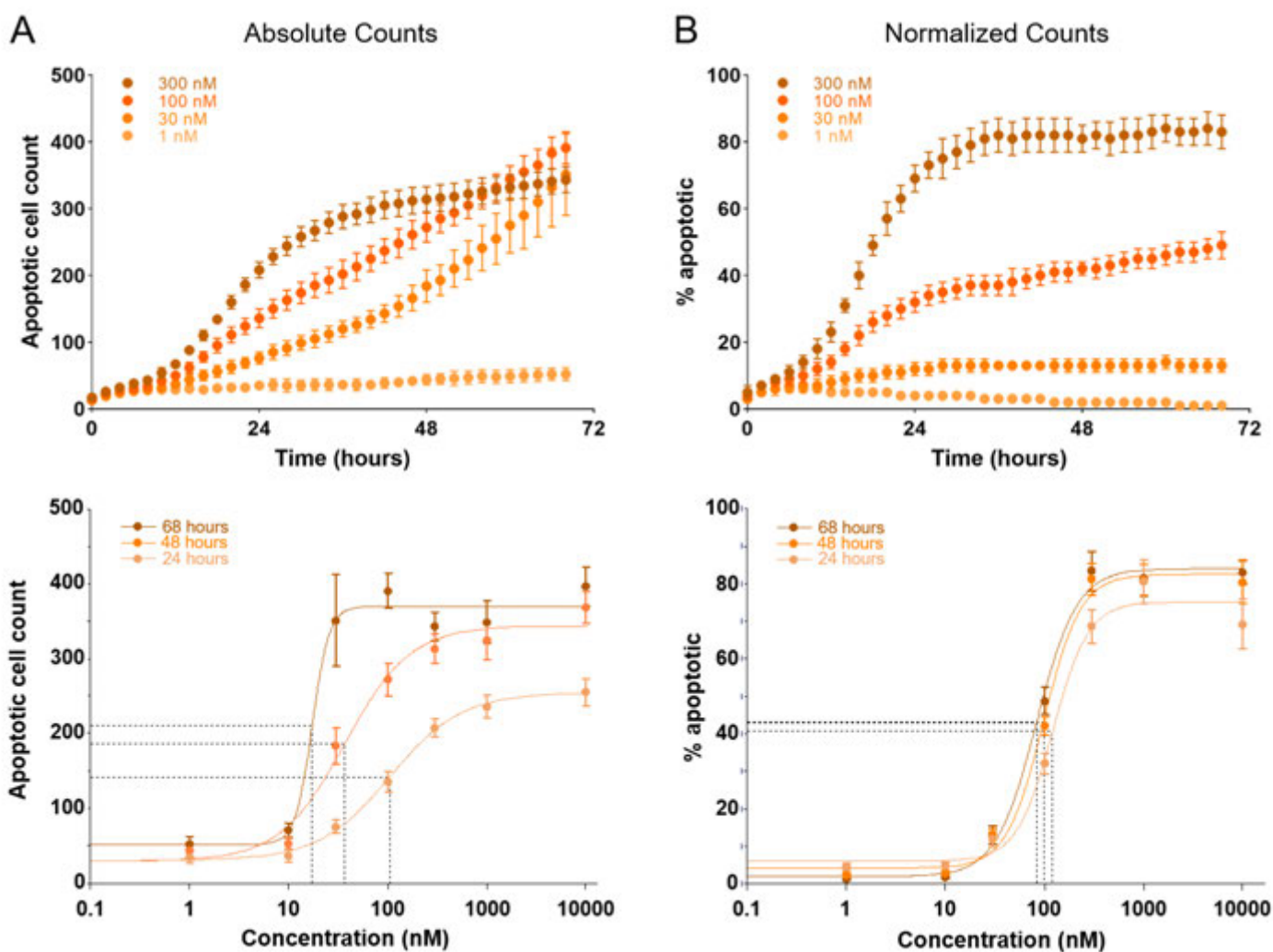


**Figure 6.** Apoptotic signal response to antineoplastics. (A) Apoptotic cell counts for the drug nocodazole applied at the four concentrations indicated. Note that apoptotic cell counts continue to rise for intermediate concentrations due to total cell counts increasing. For absolute cell counts, dose-response curves were generated and fit to the three time points indicated.  $EC_{50}$  values were substantially left-shifted over time due to cell proliferation ( $EC_{50}$  24 hours = 106 nM,  $EC_{50}$  48 hours = 30 nM,  $EC_{50}$  68 hours = 17 nM). (B) The same data for apoptotic cell counts from panel A, but normalized to total cell counts (expressed as percent). For normalized apoptotic cells, all dose-response curves consistently resulted in an  $EC_{50}$  value of approximately 100 nM. For both A and B lower panels, Agilent BioTek Gen5 4-parameter fit lines are shown in solid colors, and  $EC_{50}$  interpolation lines are shown as dashed.

Importantly, normalizing apoptotic counts to total cell counts demonstrates that the percent of apoptotic cells remains stable at a given drug concentration, despite absolute increases in both label-free cell counts and pSIVA positive counts (Figure 6B, top panel). Furthermore,  $EC_{50}$  values at different time points are stable over time, and nearly identical for normalized counts (Figure 6B, bottom panel). Therefore, quantification of the apoptotic fluorescence signal based solely on absolute counts systematically and substantially underestimates the  $EC_{50}$  value over time when cells at intermediate drug concentrations continue to proliferate.

### Quantitative analysis of necrosis

The kinetic apoptosis kit includes propidium iodide (PI) as a reporter of necrosis and late apoptosis. PI enters the cell and intercalates DNA when both the cellular and nuclear membranes are compromised; membrane integrity is lost both during late apoptosis and necrosis processes. Here, PI binding is monitored and quantified through fluorescence imaging. As with the pSIVA signal, PI signals generally increase over time and with increased drug dosage, as

shown for nocodazole (Figure 7A). As is also seen with the pSIVA apoptosis signal, the PI positive cells also increase at intermediate drug concentrations due to proliferation. Therefore, PI positive cells were also normalized as a percent of total cells using label-free cell counts (Figure 7B).

For comparison and quantitation of drug efficacy, kinetic analysis and curve fitting was performed for normalized necrosis and apoptosis signals for all drugs at 24 hours (Figure 8). Interestingly, despite nigericin's efficacy in inhibiting proliferation ( $IC_{50} = 100$  nM, see Figure 4C), it resulted in little apoptosis or necrosis at even the highest concentrations used, and  $EC_{50}$  values for apoptosis and necrosis were undetermined.

Additionally, the maximal plateau values for staurosporine reached higher levels for percent apoptosis, compared to percent necrosis, despite similarities in the  $EC_{50}$  values for both processes. This difference potentially indicates that staurosporine preferentially initiates apoptosis in HT-1080 cells. Therefore, quantitative investigation into the onset time of the apoptosis and necrosis signals was also performed using Gen5.

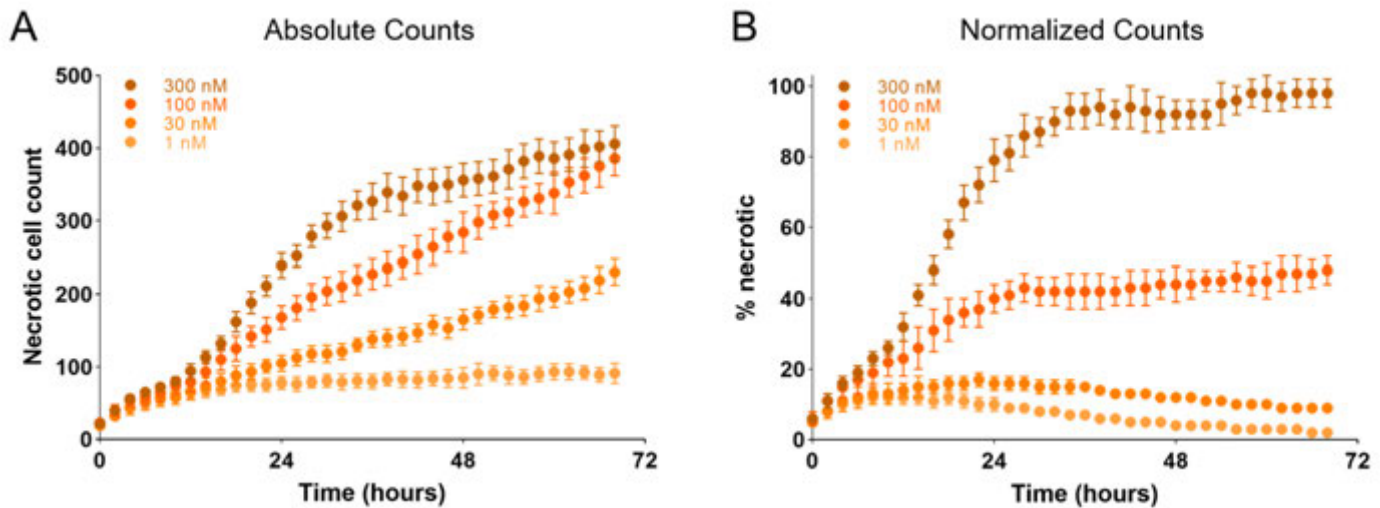


**Figure 7.** Necrotic signal response to antineoplastics. (A) Necrotic cell counts for the drug nocodazole applied at the four concentrations indicated. Note that necrotic cell counts continue to rise for intermediate concentrations due to total cell counts increasing. (B) The same data for apoptotic cell counts from panel A, but normalized to total cell counts (expressed as percent).

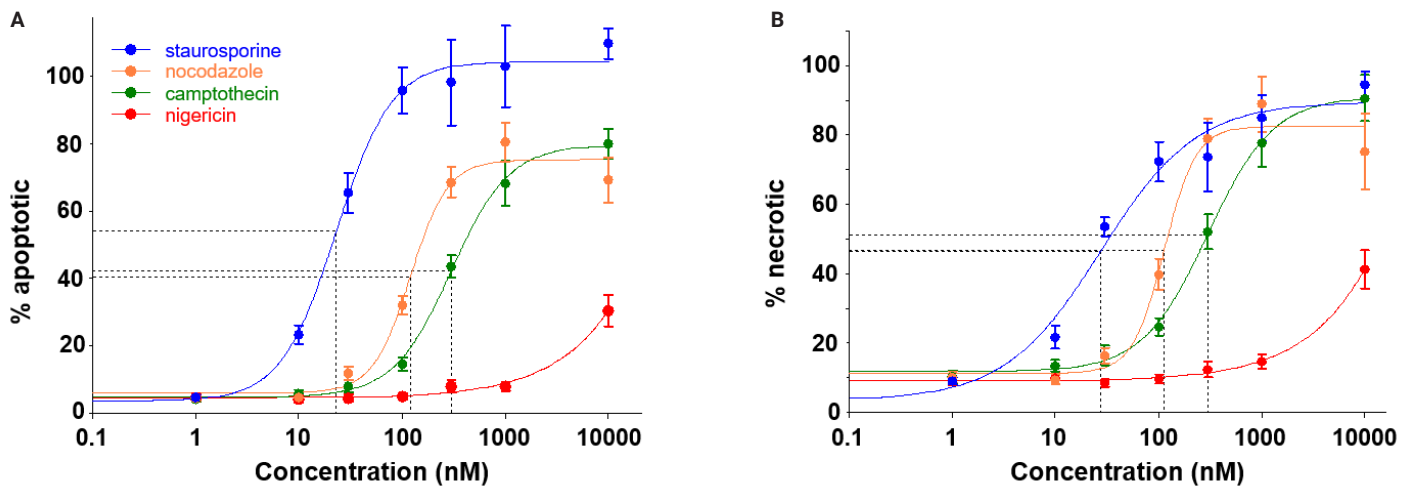


**Figure 8.** EC<sub>50</sub> determination for apoptosis and necrosis. Dose-response curves for percent necrotic (left panel) and percent apoptotic cells plotted for each drug indicated. Agilent BioTek Gen5 4-parameter fits are shown for each fit (solid colored lines) as well as interpolated EC<sub>50</sub> values (dashed lines). For apoptosis, EC<sub>50</sub> values correspond to 24 nM for staurosporine, 121 nM for nocodazole and 301 nM for camptothecin. For necrosis, EC<sub>50</sub> values correspond to 28 nM for staurosporine, 114 nM for nocodazole, and 301 nM for camptothecin. EC<sub>50</sub> values for nigericin (red) were undetermined for both apoptosis and necrosis.

In Figure 9, panel A, traces of percent apoptosis and percent necrosis are both shown for staurosporine (blue) and camptothecin (green). By eye, for cells treated with staurosporine the apoptosis signal precedes the necrosis signal. For comparison, the percent apoptosis and necrosis signals onset times are nearly identical for camptothecin, as both traces overlap significantly. To quantify this difference, the time of V<sub>max</sub> parameter was measured for each trace (see

Materials and methods for details). To evaluate time of V<sub>max</sub> for each drug, the first concentration approaching maximal levels of percent apoptosis and necrosis was chosen. The time of V<sub>max</sub> for each drug is shown in Figure 9, panel B. Only staurosporine showed an onset time difference between the two signals, with apoptosis preceding necrosis by ~3.5 hours. This finding indicates that the mechanism of cell death is primarily through apoptosis, leading to necrosis.

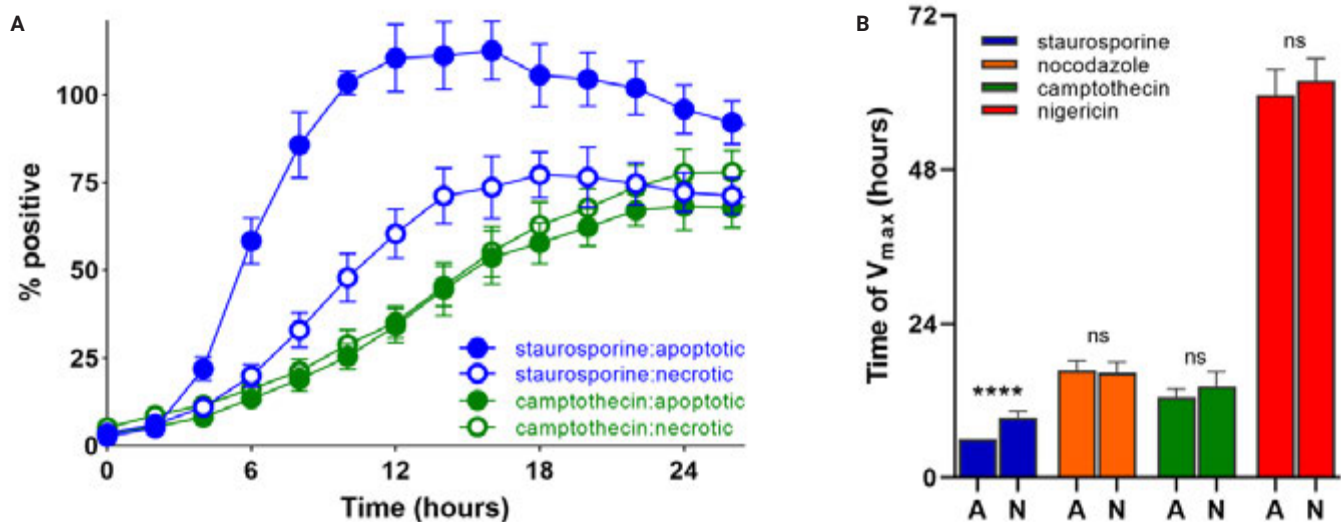


**Figure 9.** Onset time comparison for apoptosis and necrosis processes. (A) Example traces for apoptosis signal (filled circles) and necrosis signal (open circles) plotted together for the same cell population. For staurosporine (blue traces), but not camptothecin (green traces), apoptosis precedes necrosis signals. (B) Plot comparing time of V<sub>max</sub> parameter for apoptosis (abbreviated as "A") and necrosis (abbreviated as "N"). Only staurosporine showed a significant ( $p = 0.000001$ ) difference between time of V<sub>max</sub>, with apoptosis occurring ~3.5 hours earlier than necrosis.

## Conclusion

The Agilent BioTek Cytation 5 cell imaging multimode reader with wide-field-of-view camera, paired with an Agilent BioTek BioSpa automated incubator, provides a fully automated and robust means of quantifying image-based assays of cell proliferation and cell death. The wide-field-of-view camera allows single image capture of whole-well culture area, minimizing image capture time and improving compatibility for small culture area vessels for high-throughput applications. Agilent BioTek Gen5 software and cell analysis routines allow for quick, automated identification of cell counts, for both brightfield and fluorescence-based images. Normalization of fluorescence signals using the label-free cell counts was critical to avoid bias in  $EC_{50}$  determination due to differences in proliferation rates between conditions.

## References

1. Hanahan, D.; Weinberg, R. A. The Hallmarks of Cancer: The Next Generation. *Cell* **2011**, *144*(5), 646–674. doi 10.1016/j.cell.2011.02.013
2. Galluzzi, L. *et al.* Molecular Mechanisms of Cell Death: Recommendations of the Nomenclature Committee on Cell Death 2018. *Cell Death and Differentiation* **2018**, *25*, 486–541. doi.org/10.1038/s41418-017-0012-4
3. Segawa, K.; Nagata S. An Apoptotic ‘Eat Me’ Signal: Phosphatidylserine Exposure. *Trends in Cell Biology* **2015**, *25* (11), 639–650. doi.org/10.1016/j.tcb.2015.08.003
4. Kim, Y. E. *et al.* Engineering a Polarity-Sensitive Biosensor for Time-Lapse Imaging of Apoptotic Processes and Degeneration. *Nature Methods* **2010**, *7*, 67–73. doi.org/10.1038/nmeth.1405
5. Clayton, J. Kinetic Proliferation Assay using Label-Free Cell Counting. *BioTek Resources* **2017**. <https://www.biotek.com/resources/application-notes/kinetic-proliferation-assay-using-label-free-cell-counting/>.

[www.agilent.com/lifesciences/biotek](http://www.agilent.com/lifesciences/biotek)

For Research Use Only. Not for use in diagnostic procedures.

RA44173.6940393519

This information is subject to change without notice.

© Agilent Technologies, Inc. 2019, 2021  
Printed in the USA, February 1, 2021  
5994-2593EN  
AN122619\_09